Ecological Complexity 10 (2012) 69–82

Contents lists available at SciVerse ScienceDirect

Ecological Complexity

journal homepage: www.elsevier.com/locate/ecocom

Estimating insect population density from trap counts

Sergei Petrovskii [a,*], Daniel Bearup [a], Danish Ali Ahmed [a], Rod Blackshaw [b]

[a] Department of Mathematics, University of Leicester, University Road, Leicester LE1 7RH, UK
[b] Centre for Agricultural and Rural Sustainability, University of Plymouth, Drake Circus, Plymouth PL4 8AA, UK

ARTICLE INFO

Article history:
Received 9 January 2011
Received in revised form 11 October 2011
Accepted 15 October 2011
Available online 29 November 2011

Keywords:
Insect monitoring
Trapping
Trap counts
Random walk
Diffusion

ABSTRACT

Trapping is commonly used in various pest insect monitoring programs as well as in many ecological field studies. Despite this, the interpretation of trap counts is challenging. Traps are effective at providing relative counts that enable comparisons but are poor at delivering information on the absolute population size. Making better use of trap data is impeded by the lack of a consistent underlying theoretical model. In this paper, we aim to overcome current limitations of trapping methods used in ecological studies through developing a theoretical and methodological framework that enables a direct estimate of populations from trap counts. We regard insect movement as stochastic Brownian motion and use two different mathematical approaches accordingly. We first use individual-based modelling to reproduce trap catch patterns and study the effect of individual movement on observed catch patterns. We then consider a 'mean-field' diffusion model and show that it is capable of revealing the generic relationship between trap catches and population density.

1. Introduction

In ecological studies, populations are usually described in terms of the population density or population size (Begon et al., 1986; Cain et al., 2011). Having these values known over a period of time, conclusions can be made about a given species, community, or ecosystem as a whole (Royama, 1982; Kot, 2001). In their turn, conclusions often lead to decision-making about, for instance, controlling or protective measures. In particular, in pest management, the information gained about pest abundance in a given field or area is then used to make a decision about pesticide application (Stern, 1973). Activities such as this can be costly and may have drastic consequences for the ecosystems. To avoid unjustified decisions and unnecessary losses, the quality of the information about the population density is therefore a matter of primary importance.

However, the population density is rarely measured straightforwardly, e.g. by direct counting of the individuals. More often, the estimates of the population density are obtained indirectly, e.g. by collecting samples and processing the sampling data using a variety of statistical tools (Cochran, 1977; Seber, 1982; Sutherland, 1996). In the case of insects, their density is often estimated based on trap counts (Thomas et al., 1998; Raworth and Choi, 2001; Perner and Schüler, 2004; Alexander et al., 2005; Holland et al., 2005; Blackshaw and Vernon, 2008; Hicks and Blackshaw, 2008). The problem is that, once the trap counts are collected, it is not always clear how to use them in order to obtain an estimate of the population density in the field.

The essence of the problem is readily seen from the following example. An insect trap is installed in a given area, e.g. in an agricultural field. After a certain time, it is emptied and all the insects caught are counted (usually, separating different species); the corresponding numbers are called the trap counts. Consider that there are K insects of a given species S caught over the time T of the trap exposure in the field. The simple questions are: (i) Can we draw any conclusion about the density of species S in a vicinity of the trap based on only this information? If this information is not sufficient, how should it be extended, i.e. by installing more traps, having more counts, or otherwise? And, finally, given larger amounts of information (e.g. series of trap counts from several traps), what approach or algorithm can we use to estimate the population density?

Surprisingly, although these are obviously very basic questions, they have never been properly addressed. Little effort has been made to extract the information about population density from trap counts *per se*. A commonly used technique to estimate the population density is based on the mark-release-recapture method (e.g. Seber, 1982), which is effective in scientific studies but is impractical for the purposes of pest monitoring where the number of traps per unit area is usually small and release of pest insects can hardly be justified. Other approaches may not use an insect's release and recapture but still use extensive grids of traps (Perner

* Corresponding author.
E-mail address: sp237@le.ac.uk (S. Petrovskii).

1476-945X/$ – see front matter © 2011 Elsevier B.V. All rights reserved.
doi:10.1016/j.ecocom.2011.10.002

and Schüler, 2004). Meanwhile, the question remains as to whether such extensive grids are really necessary and whether an estimate of the population density can be obtained based on trap counts collected by just a few or, ultimately, by just one trap.

In this paper, we use a conceptual theoretical approach to develop two mechanistic models aimed at giving a reliable estimate of the population density from trap counts. In Section 2, we describe insect movement as the stochastic process known as Brownian motion. We simulate individual insect tracks and calculate the trap counts accordingly, and consider how the trap counts depend on the main parameters such as population density and insect mobility. In particular, we show that, although the effects of density and activity on the observed trap counts are qualitatively similar, their quantitative contribution is remarkably different. In Sections 3 and 4, we use a 'mean-field' approach to describe the insect population in terms of the population density, which appears to be a solution of the diffusion equation. In order to calculate the trap counts, we develop a semi-heuristic approach to approximate the diffusive flux through the trap boundary by simple analytical expressions. We then compare the predictions of the two approaches and show that the diffusion equation is a convenient framework to describe the trap counts on average, i.e. neglecting fluctuations of purely stochastic origin. Finally, in Section 5, we summarize our main findings and show how they can be used in practice to calculate a reliable estimate of the population density from trap counts.

2. Individual-based modelling

One way to look at the dynamics of trap counts is to simulate the movement of each individual in the field. This approach is known in the literature as individual-based modelling (Turchin, 1998; Yamanaka et al., 2003; Grimm and Railsback, 2005). Below, we briefly recall its main features. For the sake of clarity, we will focus on individual movement in two spatial dimensions, i.e. on a surface. Our analysis therefore immediately applies to trapping of walking or crawling insects in a field. An extension of our approach onto a 3D case is straightforward.

2.1. Model

In their movement, most animals move along a curvilinear path or track, i.e. $\mathbf{r} = \mathbf{r}(t)$ where t is the time and $\mathbf{r} = (x, y)$ is the animal position in a 2D domain. However, a standard observation technique usually makes it possible to only record the animal position at certain moments rather than continuously over prolonged periods of time. The continuous time t thus transforms into a finite set $t_0, t_1, t_2, \ldots, t_i, \ldots$. Correspondingly, a curvilinear path is mapped into a broken line $\mathbf{r}_0, \mathbf{r}_1, \mathbf{r}_2, \ldots, \mathbf{r}_i, \ldots$ where $\mathbf{r}_i = \mathbf{r}(t_i)$ (cf. Turchin, 1998). Generally speaking, the time step $\Delta t_i = t_{i+1} - t_i$ can be different for different i. In order to avoid unnecessary complexity, here we assume that $\Delta t_i = \Delta t = const$ and does not depend on i, so that $t_i = i\Delta t$.

Consider an individual that is situated at a position $\mathbf{r}_i = (x_i, y_i)$ at time t_i. Its position at the next moment t_{i+1} can be expressed as $\mathbf{r}_{i+1} = \mathbf{r}_i + (\Delta\mathbf{r})_i$ where $(\Delta\mathbf{r})_i = (\Delta x_i, \Delta y_i)$ is the ith step along the path. In the random walk, both Δx_i and Δy_i are random variables. We assume that there is no correlation between any two subsequent steps and the statistical properties of the movement along the path do not change with time. Therefore, the properties of the movement are fully determined by the probability distribution functions for Δx and Δy, which we denote as $\phi_{\Delta x}$ and $\phi_{\Delta y}$, respectively. We consider the case that the environment is isotropic and there is no advection of any kind, so that there is no drift in any preferable direction.

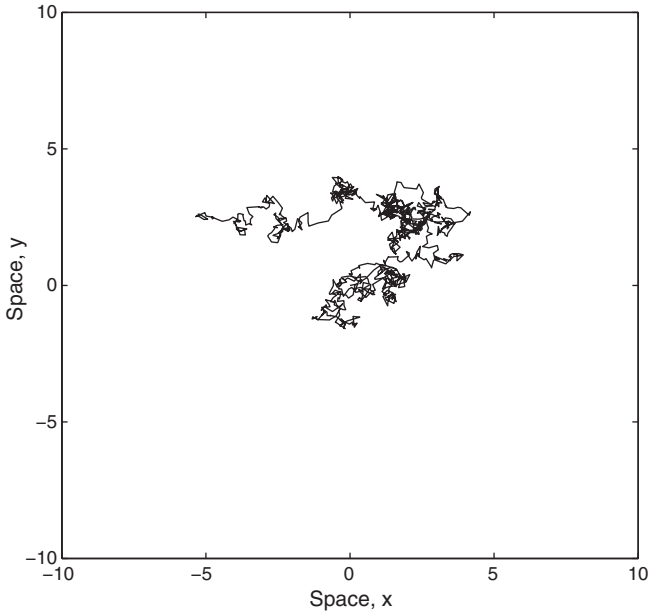

Fig. 1. A typical path of an animal performing the Brownian motion generated using Eq. (1) with $\delta^2 = 0.02$. The path consists of 1000 steps starting from the initial position at (0, 0).

Correspondingly, we consider $\phi_{\Delta x}$ and $\phi_{\Delta y}$ to be normal distributions with zero means:

$$\phi(\Delta x) = \frac{1}{\delta\sqrt{2\pi}}\exp\left[-\frac{(\Delta x)^2}{2\delta^2}\right], \qquad \phi(\Delta y) = \frac{1}{\delta\sqrt{2\pi}}\exp\left[-\frac{(\Delta y)^2}{2\delta^2}\right]. \tag{1}$$

Note that, in an isotropic environment, the variances for $\phi_{\Delta x}$ and $\phi_{\Delta y}$ should be equal, so that Eq. (1) have only one parameter δ.

For any given δ, Eq. (1) can be used to simulate the movement path; see Fig. 1. The corresponding random process is called Brownian motion. Its signature is that the mean square displacement $\langle \mathbf{r}^2(t_i)\rangle$ increases linearly with time (e.g. Turchin, 1998; Sornette, 2004), i.e., for a fixed Δt, with the number i of the steps.

Note that it depends on the time step Δt of the observations whether the assumption of the absence of correlation between any two subsequent steps is realistic or not. For a sufficiently small value of Δt, it is hardly feasible to assume that subsequent steps are uncorrelated. Indeed, in the case where the movement path is a smooth curve, the movement direction of the preceding step is a preferred direction for the next step. Therefore, the expected values of the turning angle are likely to be centered around zero. The corresponding random process is known as the Correlated Random Walk (Kareiva and Shigesada, 1983). Remarkably, however, the CRW attains the properties identical to the Brownian motion when Δt becomes sufficiently large (Kareiva and Shigesada, 1983).

2.2. Simulations

In ecological applications, there is not just one insect wandering in the field but many of them, say, N. We assume that their movement can be described as Brownian motion. Correspondingly, at each time step, the new positions for all N animals are calculated[1] using the probability distribution functions (1).

[1] Here we assume that all individuals of the given species are identical with regard to their movement abilities. The impact of individual differences can change the results significantly; see Petrovskii and Morozov (2009) and Petrovskii et al. (2011).

A trap introduces a perturbation to the movement. Once the animal's path crosses the trap boundary, the animal is trapped and the path terminates (Fig. 2). Consider a trap of circular shape with radius R and its center at $(\overline{x}, \overline{y})$. A given animal is caught at moment t_i if

$$\left[(x_i - \overline{x})^2 + (y_i - \overline{y})^2\right]^{1/2} < R \tag{2}$$

for a certain i but relation (2) does not hold for any $t_k < t_i$.

In our simulations, we consider a square-shaped domain, $-L < x < L$ and $-L < y < L$ where L is a parameter, with a circular trap installed in the middle, i.e. $\overline{x} = \overline{y} = 0$. For ecological reasons, we consider that $R \ll L$. At $t_0 = 0$ there are N insects distributed uniformly (in a statistical sense) over the domain. At each time step, after the new position for each of the insects has been simulated, the condition (2) is applied. The trap counts are obtained accordingly: when the position of an animal is first observed to be inside the trap, the corresponding path is terminated and the trap count increases by one. At the outer boundary of the domain, the no-flux condition is used so that an insect that has walked out of the domain is brought back. Therefore, the total population size can only change (decrease) because of the insects caught in the trap.

Fig. 3 shows the snapshots of the population distribution over space obtained at different time for parameters $L = 50$, $N = 10^4$ (which corresponds to the population density $n = 0.25NL^{-2} = 1$), $R = 5$, $\Delta t = 0.01$ and $\delta^2 = 0.02$). In agreement with intuitive expectations, the trap introduces a spatially inhomogeneous perturbation into the population distribution: the insect density remains unperturbed far away from the trap but it decays to a low

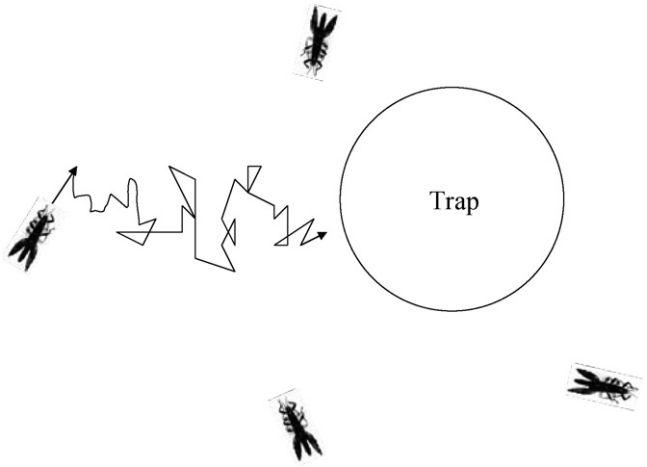

Fig. 2. A sketch of animal movement in vicinity of a trap.

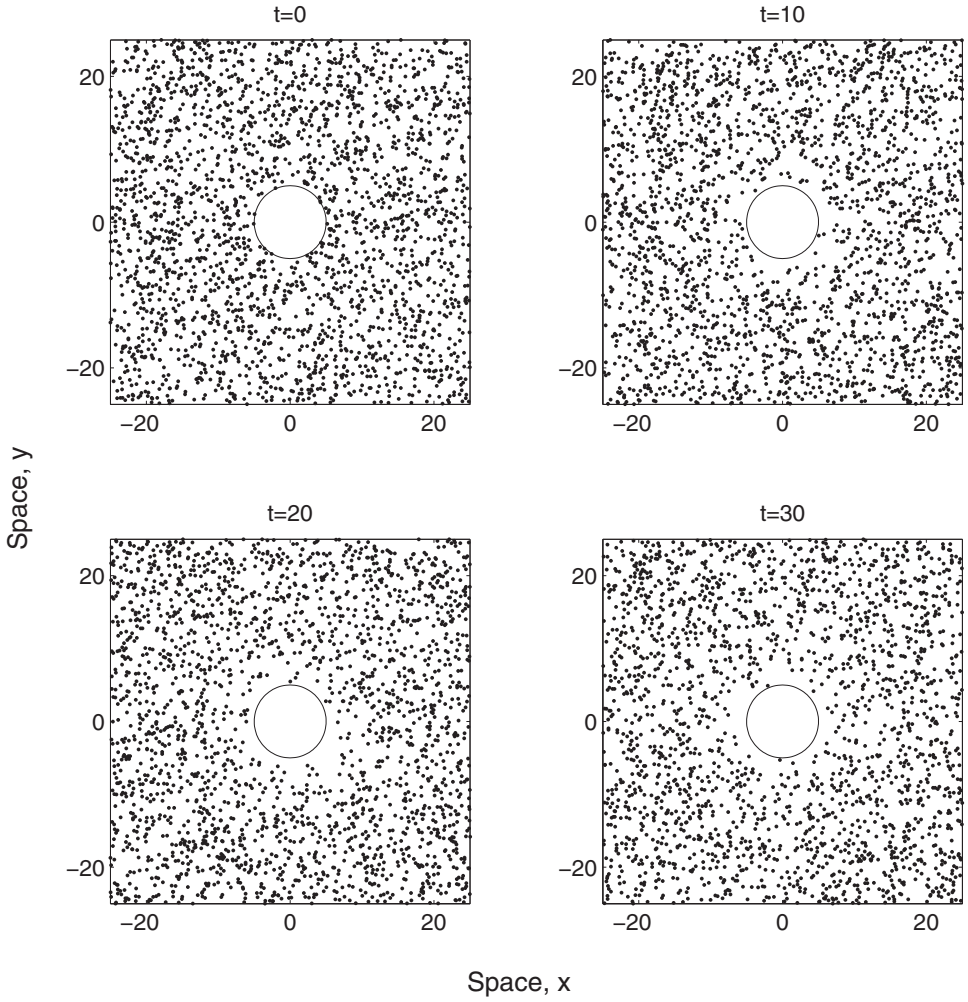

Fig. 3. Snapshots of the population distribution over space shown after 0, 1000, 2000 and 3000 time steps (left to right, top to bottom, respectively). Parameters are $n = 1$, $L = 50$ (only a part of the domain is shown), $R = 5$, $\Delta t = 0.01$ and $\delta^2 = 0.02$.

value near the trap boundary. The radius of the perturbed area clearly grows with time, cf. top and bottom panels in the right column of Fig. 3.

It is readily seen that this emerging spatial pattern has an immediate effect on the trap counts. Indeed, for any given level of insects activity (i.e. for any given δ), it is obvious that the larger the population density in vicinity of the trap is the greater the number of insects caught per unit time. Therefore, on average (up to fluctuations of stochastic origin, see below), the number of insects caught per unit time should decrease monotonously with time. Correspondingly, one can expect that the graph showing dependence of trap counts against time should be a convex curve.

This heuristic argument appears to be in full agreement with simulation results. Fig. 4a shows the trap count vs. time calculated over 3000 steps (parameters are the same as in Fig. 3). The somewhat jagged shape of the curve is the result of stochastic fluctuations due to the finiteness of the population. To decrease the impact of stochasticity, we have repeated the simulations 10 times, each simulation run corresponding to a different realization of the random process, and averaged the results. The average trap count is shown in Fig. 4c; the curve has become much smoother.

Note that, from an ecological point of view, averaging over different simulation runs is equivalent to averaging over the data collected from different traps installed in the same field, provided there is not much variation in the population density and environmental factors between different traps and that the traps are installed not too close to each other so as to avoid the overlapping of the perturbation zones. Therefore, this procedure to decrease the effects of stochasticity is relatively straightforward to incorporate into an ecological protocol.

A close inspection of Fig. 3 shows that the size of the perturbed zone grows with a finite speed and, in fact, rather slowly. It means that, if the time of trap exposure is not large, the perturbation may not reach the outer boundary of the domain. Therefore, over the time of trap exposure, the boundary will not have any significant effect on the population's spatial distribution in the vicinity of the trap. In turn, this means that the details of the boundary shape are not important; for instance, the trap counts obtained in a circular-shaped field and in a square-shaped field should exhibit similar patterns.

This prediction is confirmed by the simulation results. The blue curve in Fig. 4c is obtained by averaging the counts over 10 simulation runs for a circular domain of radius L. Apparently, at least up to $t = 20$ days the two curves lie very close to each other.

Fig. 4a and c shows the number of caught insects as it accumulates in the trap in the course of time. The trap count calculated in this way is a non-decreasing function of time. However, the ecological data obtained in applications using traps are usually collected in a somewhat different way. The traps are emptied periodically, e.g. daily or weekly, the number of the

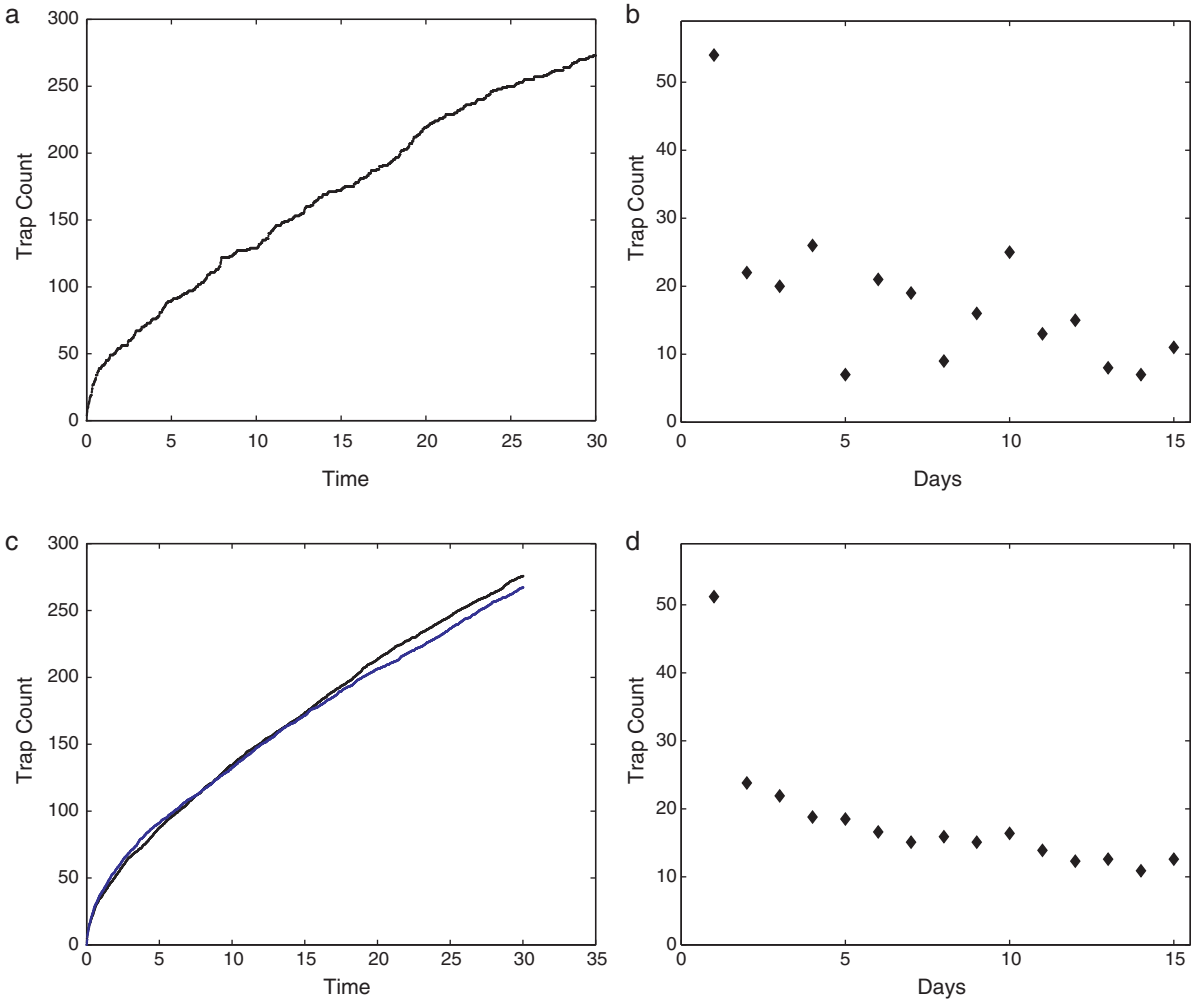

Fig. 4. Trap counts vs. time (in days) obtained for $n = 1$: (a) the cumulative number of insects caught; (b) daily trap counts; (c) and (d) the same as in (a) and (b), respectively, but with the trap counts averaged over 10 simulation runs. The blue curve in (c) shows the average trap counts obtained for a domain of circular shape (see details in the text). Parameters are the same as in Fig. 3.

insects caught over the period of trap exposure is recorded and is called a daily (or weekly) trap count. Correspondingly, the trap count for the next period of trap exposure always starts from zero. Fig. 4b show the simulation data of Fig. 4a presented in this way (in abstract time units, considering 1 day = 200 time steps). Interestingly, although the effect of stochastic fluctuations is apparently not significant in Fig. 4a, it becomes very clear in daily counts. Although the daily counts tend to decrease with time (as can be expected from the convex shape of curve in Fig. 4a), interpretation of any subset of the data can be misleading. For instance, the daily counts obtained from day 8 to 10 show a significant increase. However, this has nothing to do with a change of the population density, being just a result of inherent stochastic fluctuations. Therefore, if considered out of the context, such a short-time increase can give a completely incorrect impression.

Note that these fluctuations in the daily counts can be suppressed if, as above, the results are averaged over several realizations of the system's dynamics, i.e. over several simulation runs. Fig. 4d show the daily counts after averaging over 10 simulation runs. The fluctuations have become much smaller.

The results shown in Fig. 4 are obtained for the number of insects $N = 10^4$, which corresponds, for the given size $L = 50$ of the domain, to the population density $n = 1$. Recalling that the trap radius $R = 5$, this density can be regarded as rather high. In pest control practice, the pest density is usually low. An important question is therefore how the results change for smaller values of n. A generic property of an N-particle stochastic system is that the relative magnitude of stochastic fluctuations is proportional to $N^{-1/2}$ (e.g. Balescu, 1975). Correspondingly, one can expect stochastic fluctuations to become more prominent for smaller values of n.

Fig. 5 shows the trap counts obtained for $n = 0.1$, other parameters being the same as in Fig. 4. The impact of fluctuations on the cumulative trap counts has now become notably stronger resulting in a very jagged curve shown in Fig. 5a. Averaging over 10 simulation runs makes the curve smoother (see Fig. 5c) but its shape remains distorted compared to the previous case of $n = 1$. A similar observation can be made about the daily counts; averaging decreases the magnitude of fluctuations, cf. Figs. 5b and d, but the pattern in the daily counts that was readily seen for $n = 1$ (Fig. 4d) is now considerably distorted.

The impact of the fluctuations becomes much larger for $n = 0.01$; see Fig. 6a and b. Averaging over 10 simulation runs does not bring back the trap counts' generic properties observed in the high density case (shown in Fig. 4c and d): the cumulative trap count vs. time (Fig. 6c) is not a smooth curve any more and the daily counts (Fig. 6d) do not show any sign of pattern.

An interesting question is how trap counts depend on individual mobility, i.e. on the variance δ^2 of the step size distribution. In particular, our approach makes it possible to have an insight into the activity-density problem (Thomas et al., 1998), i.e. to what extent a decrease in the insect density can be

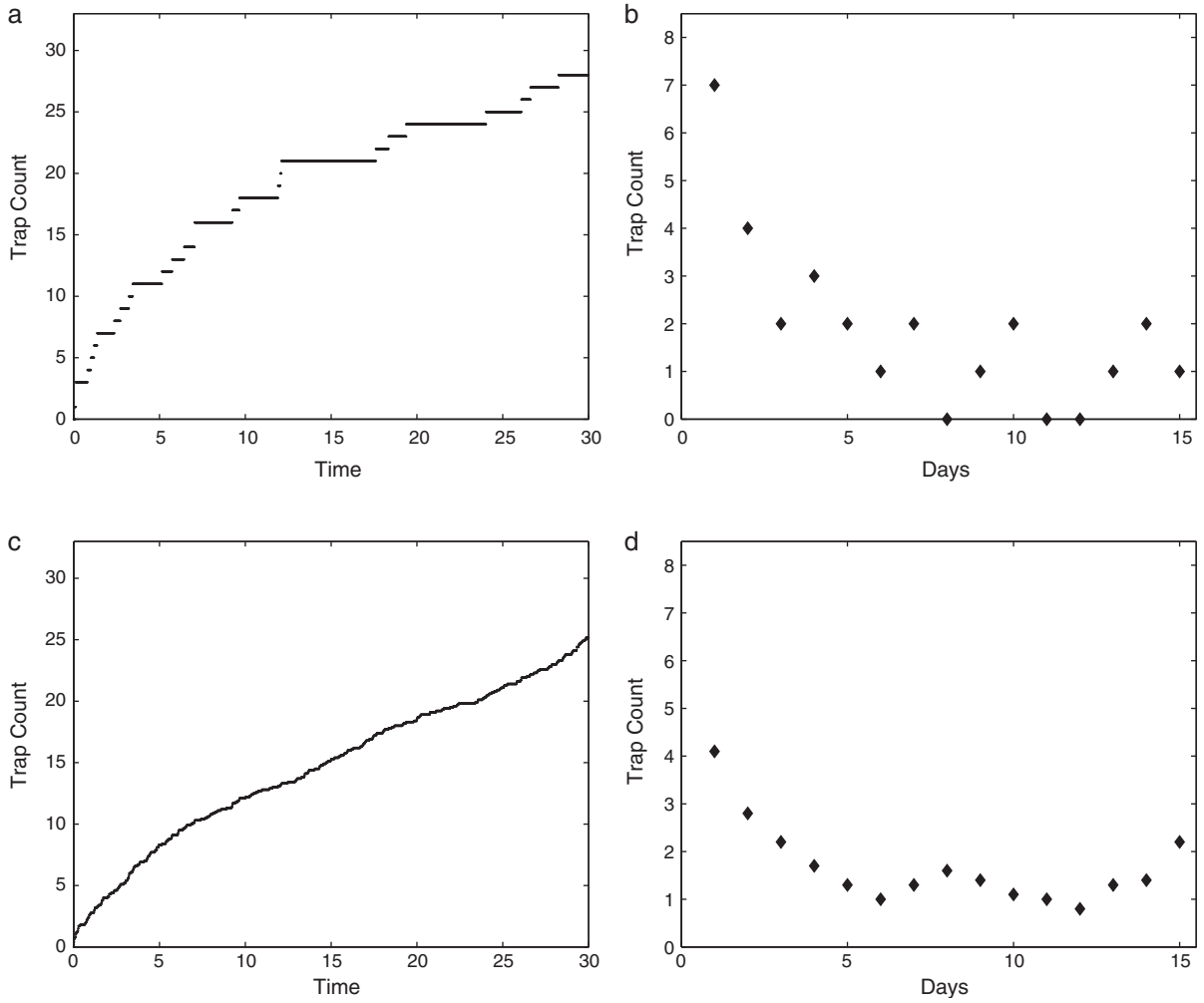

Fig. 5. Trap counts vs. time (in days) obtained for $n = 0.1$, other parameters are the same as in Figs. 3 and 4: (a) the cumulative number of insects caught; (b) daily trap counts; (c) and (d) the same as in (a) and (b), respectively, but with the trap counts averaged over 10 simulation runs.

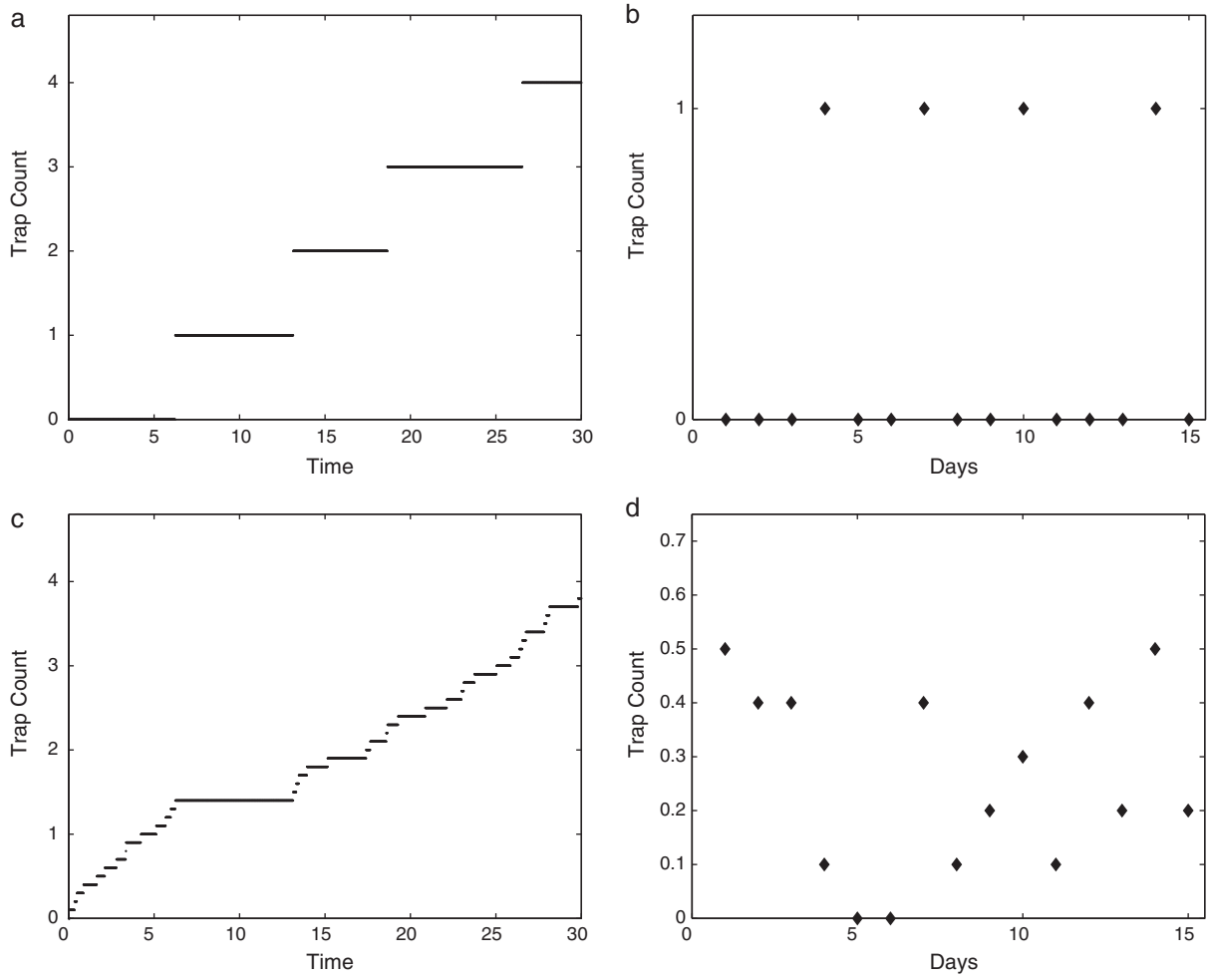

Fig. 6. Trap counts vs. time (in days) obtained for $n = 0.01$, other parameters are the same as in Figs. 3 and 4: (a) the cumulative number of insects caught; (b) daily trap counts; (c) and (d) the same as in (a) and (b), respectively, but with the trap counts averaged over 10 simulation runs.

compensated by an increase in their mobility and whether this compensation can result in the same trap counts. Indeed, intuitively, a possibility of such compensation seems obvious: an individual 'particle' (insect) with a higher mobility would browse, per unit time, over a larger area and hence would have a larger probability of being trapped. This larger probability for a single randomly walking individual turns into larger trap counts in the case of a multi-particle system. However, the quantitative aspects of the activity-density relation are understood rather poorly. A practically important question is as follows: if the insect density falls, say, m times, how large should the corresponding increase in the individual mobility be to result in the same trap counts?

In order to address this issue, we compare the cases with $n = 0.1$ and $n = 0.01$ (see Figs. 5 and 6, respectively); therefore, $m = 10$. We run simulations with $n = 0.01$ for different values of δ^2 to obtain the cumulative trap count dynamics similar to that shown in Fig. 5a. Interestingly, contrary to intuitive expectations, the 10-fold increase in δ^2 leads to much lower values in the trap counts; see Fig. 7(top) obtained for $\delta^2 = 0.2$. A 100-fold increase in δ^2 leads to much higher trap counts; see Fig. 7(middle) obtained for $\delta^2 = 2$. By a trial and error approach, we have found that the required increase in δ^2 should be 30 times. Fig. 7(bottom) shows the cumulative trap counts vs. time obtained for $\delta^2 = 0.6$; it is readily seen that it agrees very well with the results shown in Fig. 5a.

We therefore conclude that, although our results do confirm the heuristic 'activity-density' concept qualitatively, predicting that the effects of the population density can be made equivalent to the effects of the individual mobility, the actual relation appears to be somewhat counter-intuitive. In order to compensate a 10-fold decrease in the insect density, the individual mobility must increase 30 times, where the factor 30 can hardly be obtained from heuristic arguments.

3. Mean-field approach: diffusion equation

The individual-based approach used in the previous section makes it possible to simulate the trap counts directly. Therefore, it is very useful in the sense that it makes it possible to mimic a specific situation in real-world pest control. However, since this approach is essentially simulation-based, it does not allow us to make any general conclusions about trap counts for different parameter values.

There is, however, another approach. It is well known (e.g. Okubo, 1980; Berg, 1983; Turchin, 1998; Sornette, 2004; Chorin and Hald, 2006) that the population density $u(x, y, t)$ of a system of particles performing Brownian motion is a solution of the diffusion equation:

$$\frac{\partial u(x,y,t)}{\partial t} = D\nabla^2 u(x,y,t), \tag{3}$$

subject to appropriately chosen initial and boundary conditions. Here D is the diffusion coefficient which is related to the parameters of individual movement (see Section 2.1) by the

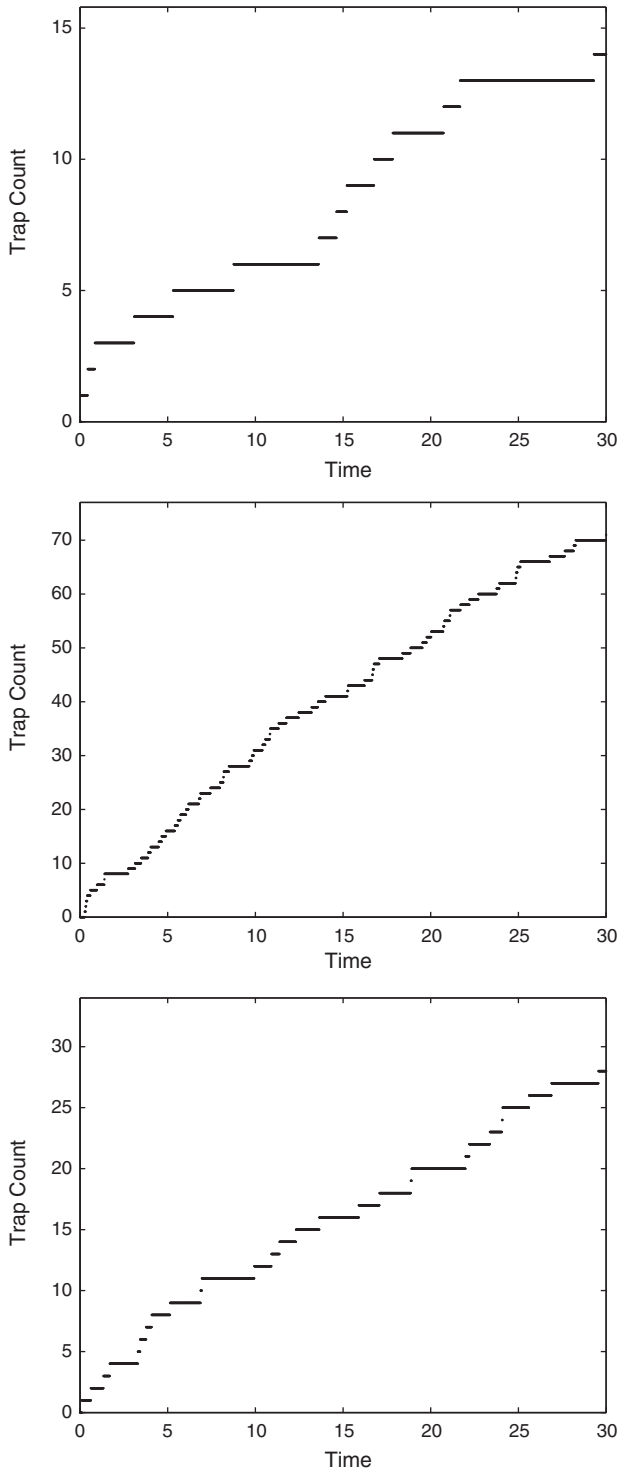

Fig. 7. Cumulative trap counts vs. time for different values of the individual mobility: (top) $\delta^2 = 0.2$, (middle) $\delta^2 = 2.0$, (bottom) $\delta^2 = 0.6$. The insect density $n = 0.01$, other parameters the same as above.

following equation:

$$D \approx \frac{\delta^2}{2\Delta t}. \tag{4}$$

Relation (4) becomes an exact equality when both Δt and δ^2 tend to zero (Okubo, 1980; Sornette, 2004).

Note that, although the Brownian motion is an essentially stochastic process, the diffusion equation describes it in a deterministic way. Correspondingly, it does not take into account fluctuations explicitly. Also, it is only valid on a spatial scale much larger than the scale of the individual walk. For these reasons, the approach based on the diffusion equation is called a mean-field description. Fig. 8 shows the trap counts vs. time calculated in a circular domain with a circular trap using the diffusion equation (green curve) and the individual-based simulations (blue curve). Clearly, the agreement between the two approaches is very good.

The agreement between the two approaches showed in Fig. 8 is partially ensured by considering the case of large insect density. As previously noted, a fundamental result of statistical mechanics (e.g. see Balescu, 1975) is that the relative magnitude of stochastic fluctuations decreases as $N^{-1/2}$ where N is the population size. Indeed, the magnitude of fluctuations in individual-based results shown in Fig. 8 is almost negligible. In the case of a smaller population density, the fluctuations can become much more prominent. In this case, as will be shown below, the mean-field approach can still be applicable to describe the trap counts in terms of averaged values.

In practical applications concerned with trapping of walking or crawling insects, the diffusion equation should be considered on a 2D domain (on a 3D domain for flying insects). However, it is instructive to begin with an 1D case when the population density depends on one spatial coordinate only:

$$\frac{\partial u(x,t)}{\partial t} = D\frac{\partial^2 u(x,t)}{\partial x^2}, \tag{5}$$

where $-L < x < L$. We assume that insects cannot leave the domain or immigrate from the outside, i.e. there is no population flux through the domain's boundary:

$$\frac{\partial u(x,t)}{\partial x} = 0 \quad \text{for } x = \pm L. \tag{6}$$

Consider the case when an escape-proof trap of size l is installed in the middle of the domain. Correspondingly, $u(x,\ t) \equiv 0$ for $-l < x < l$, which means that the following condition holds at the trap boundary:

$$u(-l,t) = u(l,t) = 0. \tag{7}$$

For the initial conditions, we consider the case when the population is distributed uniformly around the domain:

$$u(x,0) = n = \text{const} \quad \text{for } l < |x| < L. \tag{8}$$

From the point of a two-dimensional system, the problem ((5)–(8)) describes a long slot-like trap going across the whole field, thus dividing it into two unconnected parts. Although this situation is hardly practical, the solution of ((5)–(8)), as we will show below, appears to be useful in a more realistic geometry of a circular or square-shaped trap.

The problem ((5)–(8)) can be solved analytically using the separation of variables method (see Appendix A). Note that it is sufficient to solve the problem for $l < x < L$. It is then convenient to redefine the spatial domain as $\xi = x - l, 0 < \xi < \tilde{\mathcal{L}} = L - l$. The solution is shown in Fig. 9 at different time t. It is readily seen that the trap introduces a perturbation into the otherwise spatially uniform population distribution, which is in agreement with the results of the individual-based modelling, cf. Fig. 3.

We want to mention that the diffusion equation is known to possesses self-similarity (e.g. see Barenblatt, 1996), which means that its solutions taken at two different times can be mapped into each other[2] by using the scaling factor $\sqrt{Dt}$. For the diffusion

[2] Under some restrictions on the system's geometry and the initial conditions.

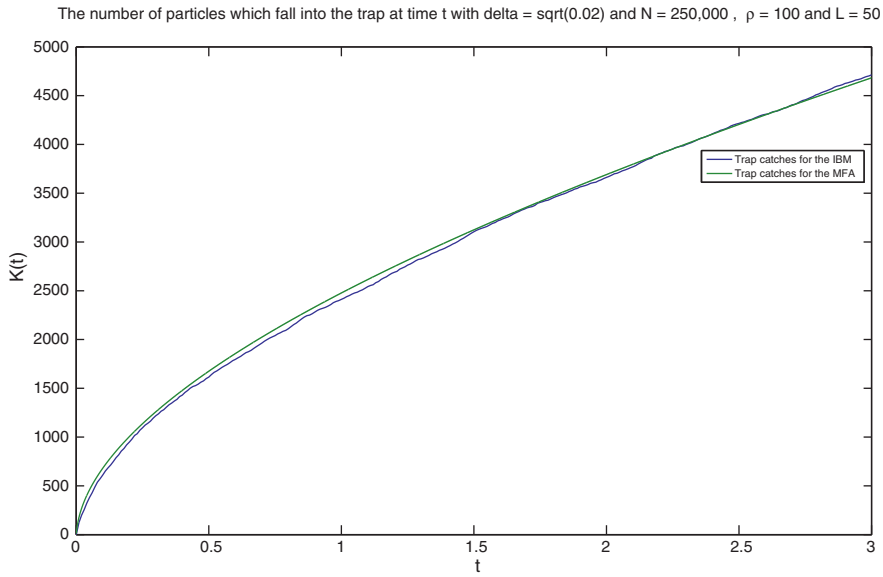

Fig. 8. Comparison between the mean-field approach and individual-based modelling. The two curves show trap count vs. time; the green curve is obtained using the diffusion equation and the blue curve is obtained using individual-based simulations. Parameters are $n = 100$, $D = 1$, $\delta^2 = 0.02$ and $R = 3.2$. (For interpretation of the references to color in this figure legend, the reader is referred to the web version of the article.)

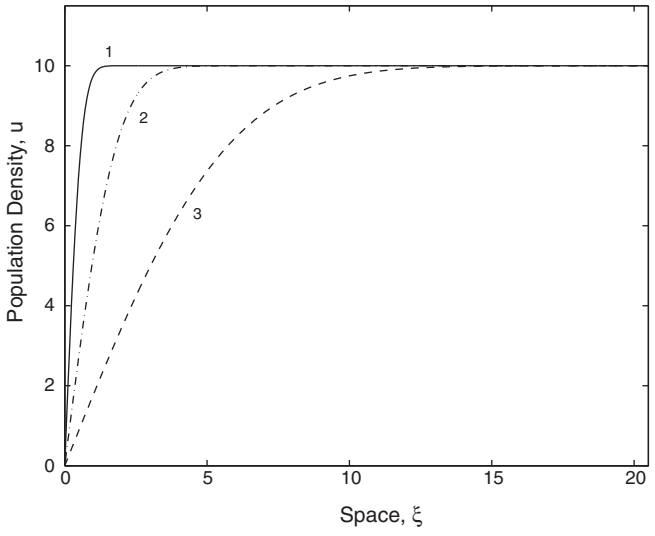

Fig. 9. Population density vs. space as given by the solution of the diffusion problem ((5)–(8)) at $t = 0.1$ (solid curve 1), $t = 1$ (dashed-and-dotted curve 2) and $t = 10$ (dashed curve 3) for parameters $D = 1$, $n = 10$ and $\tilde{\mathcal{L}} = 30$.

problem ((5)–(8)), $\sqrt{Dt}$ gives a width of the perturbation area near the trap boundary.

Once the solution is known, the corresponding trap count over time t can be obtained as

$$(\Delta N)_t = \int_0^t j(\tau)d\tau, \tag{9}$$

where $j(t)$ is the diffusive flux of the population density through the trap boundary.

Note that the exact analytical solution of the problem ((5)–(8)) is given in the form of an infinite series and therefore the expression for $(\Delta N)_t$ is an infinite series as well. An infinite series is not very convenient to work with. However, it appears that the trap count can be calculated as

$$(\Delta N)_t \approx \frac{2n}{\sqrt{\pi}}\sqrt{Dt} \tag{10}$$

with a very good accuracy unless t is very large; see Appendix B for details.

4. Diffusion equation in two spatial dimensions

We now consider the diffusion equation (3) in a more realistic case of a 2D domain. The first question to be addressed is the importance of the trap shape. We consider two special cases, i.e. when (i) the trap is of circular shape and (ii) the trap is of square shape. Correspondingly, the diffusion equation has to be solved in domains Ω_c and Ω_s that can be formally described as

$$\Omega_c = \{(x,y) : |x| < L, |y| < L, x^2 + y^2 > R^2\}, \tag{11}$$

where R is the trap radius, and

$$\Omega_s = \{(x,y) : l < |x| < L\} \bigcup \{(x,y) : l < |y| < L\}, \tag{12}$$

where l is the trap size.

On the domain's boundary, we consider the zero-flux condition:

$$\left.\frac{\partial u(x,y,t)}{\partial x}\right|_{x=\pm L} = \left.\frac{\partial u(x,y,t)}{\partial y}\right|_{y=\pm L} = 0. \tag{13}$$

At the trap boundary, we consider the zero-density condition, i.e., respectively,

$$u(x,y,t) = 0 \quad \text{for } x^2 + y^2 = R^2 \tag{14}$$

in the case of (11) and

$$u(x,y,t) = 0 \quad \text{for } x = \pm l, |y| < l \text{ and } y = \pm l, |x| < l \tag{15}$$

in the case of (12).

For the initial conditions, we consider that the population density is distributed homogeneously over the space:

$$u(x,y,0) = n = \text{const} \quad \text{for} (x,y) \in \Omega_{c,s}. \tag{16}$$

Eq. (3) for both cases (i) and (ii) is solved numerically.[3] The corresponding trap counts are shown in Fig. 10. We therefore

[3] A formal solution of the diffusion problem in the case of cylindrical symmetry can be found by the separation of variables method; however, it is not useful for practical purposes because the coefficients in the series contain zeros of the Bessel functions that are not known analytically (Crank, 1975).

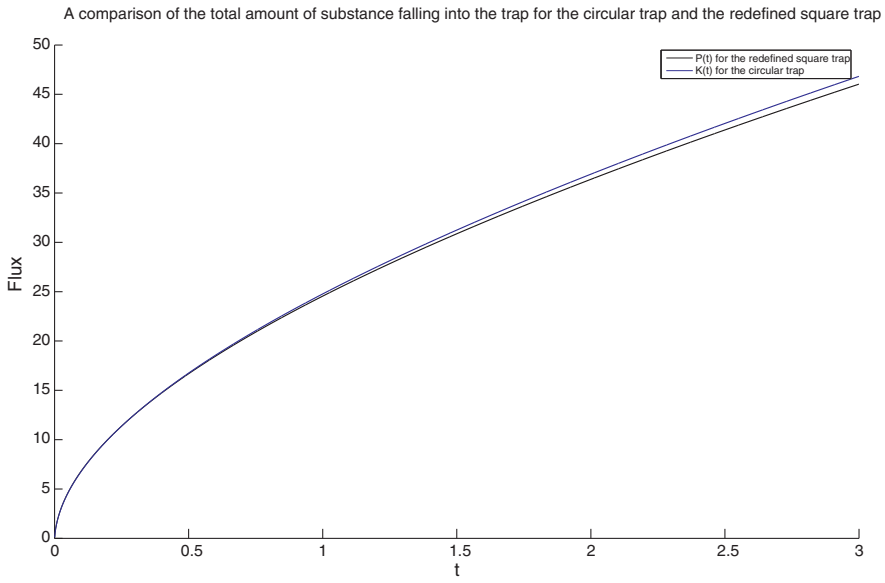

Fig. 10. Comparison of trap counts for two traps of different shape with the same perimeter $p = 20$, black curve for the square-shaped trap, blue curve for the circular trap. Other parameters are $D = 1$, $L = 10$ and $n = 1$. (For interpretation of the references to color in this figure legend, the reader is referred to the web version of the article.)

observe that the trap counts do not depend much on the details of the trap shape. Although this may not necessarily be true for traps of a more complicated shape (e.g. star-like or cross-shaped), in case of the square trap and the circular trap the difference between the two solutions is negligibly small. In particular, it means that the impact of the corners in the case of square geometry is not important.

We also considered the effect of the field's shape by solving the diffusion equation numerically in a square domain and in a circular-shaped domain. In full agreement with the results of the individual-based modelling of Section 2, see Fig. 4c, our simulation results (not shown here for the sake of brevity) confirm that trap counts do not depend on the field's shape until t becomes very large, i.e. until the trap-induced perturbation reaches the field boundary.

One technical problem that arises in the 2D case is that the solution of the diffusion equation is either given by a bulky infinite series or is obtained numerically. In both cases, it is difficult to reveal the generic solution dependence on the parameters. In order to address this problem, one can try to make use of the solution obtained in the 1D case, where the trap catches can be approximated by a very simple analytical formula (10). We will call this approach the quasi-1D approximation. The idea is sketched in Fig. 11. We first assume that the diffusion flux through each of the sides of the square-shaped trap can be described as the 1D flux (see arrow A) multiplied by the side length l. Correspondingly, the trap count in a 2D domain with a square-shaped trap is calculated as

$$(\Delta N)_t^* \approx p(\Delta N)_t, \tag{17}$$

where $(\Delta N)_t$ is given either by the exact solution (27) or by its approximation (10), and $p = 4l$ is the trap perimeter.

However, a straightforward application of this idea leads to a rather poor result; see the black solid curve in the left part of Figs. 12 and 13. Although it does describe the trap counts very well at small t (up to $t \approx 3$), it significantly under-estimate them at an intermediate or large t. A closer look at the system's geometry immediately reveals the reason. The quasi-1D approximation of the 2D diffusive flux only takes into the account the population that is within the cross-like area (shown by dotted straight lines in Fig. 11) centered at the trap. This may be a reasonable approximation at small t when the shape of the perturbed region more or less follows the shape of the trap (see curve 1); however, diffusion will eventually smooth down the corners so that, at a large t, the shape of the perturbed region is close to circular (curve 3). The insects diffusing towards the trap now come from this larger area (see arrow B) but Eq. (17) only takes into account the density inside the cross-like region.

In order to take this into account, we make a heuristic extension of Eq. (17) by rescaling the area involved into the diffusive transport:

$$(\Delta N)_t^* \approx p(\Delta N)_t \left(1 + \kappa \frac{A_{tot}(t)}{A_{cr}(t)}\right), \tag{18}$$

where p is the trap perimeter, $A_{cr}(t)$ is the area affected by the diffusion inside the cross-like region, $A_{tot}(t)$ the total area affected and κ is a numerical coefficient on the order of unity. At $t \gg 1$, when the change of shape of the perturbed region becomes important, we expect that $A_{tot}(t) \gg A_{cr}(t)$. Indeed, if we denote the

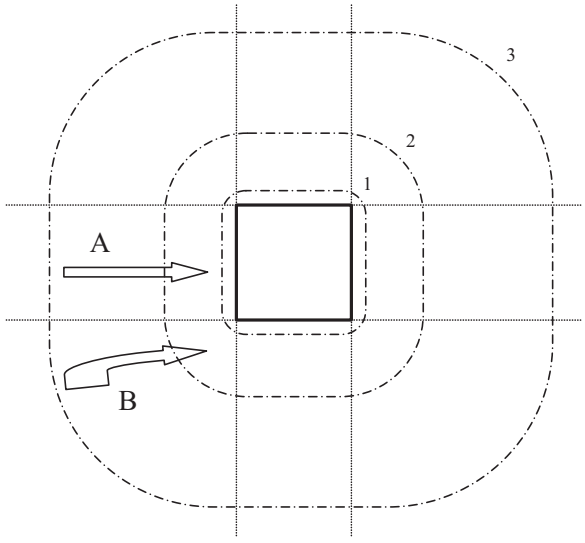

Fig. 11. A sketch of spatial perturbation growth around a square-shaped trap (thick line). Arrows indicate the diffusive flow towards the trap, the dashed-and-dotted curves show the boundary of the perturbed area for $t_3 > t_2 > t_1$.

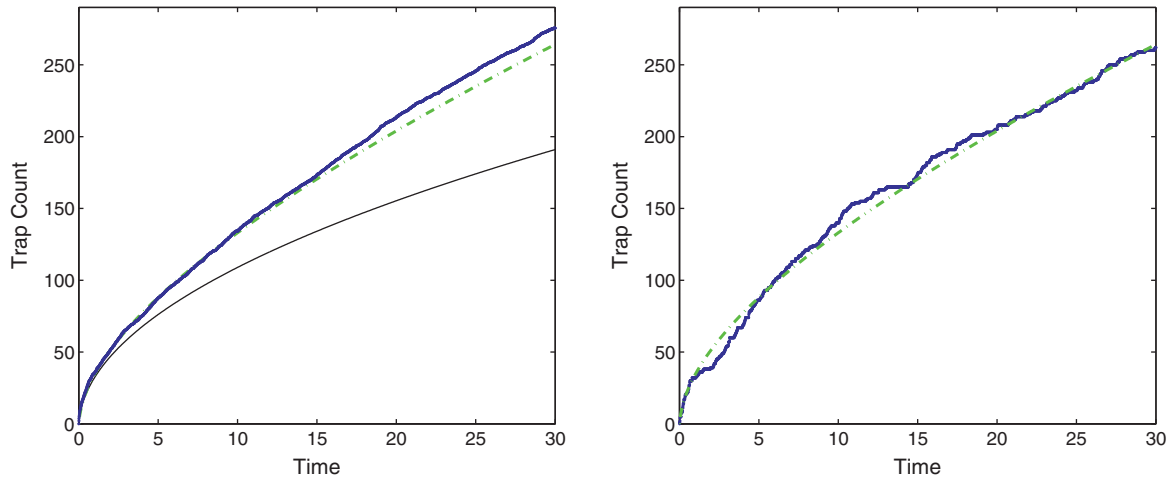

Fig. 12. Trap counts calculated using the individual-based approach (thick blue solid curve) and the scaled mean-field approach (green dashed-and-dotted curve), see Eq. (19): (left) averaged over 10 stochastic realizations, (right) for a typical stochastic realization. Parameters are $D = 1$, $n = 1$, $L = 50$ and $\kappa = 0.7$. The black solid curve shows the unscaled mean-field result given by (17). (For interpretation of the references to color in this figure legend, the reader is referred to the web version of the article.)

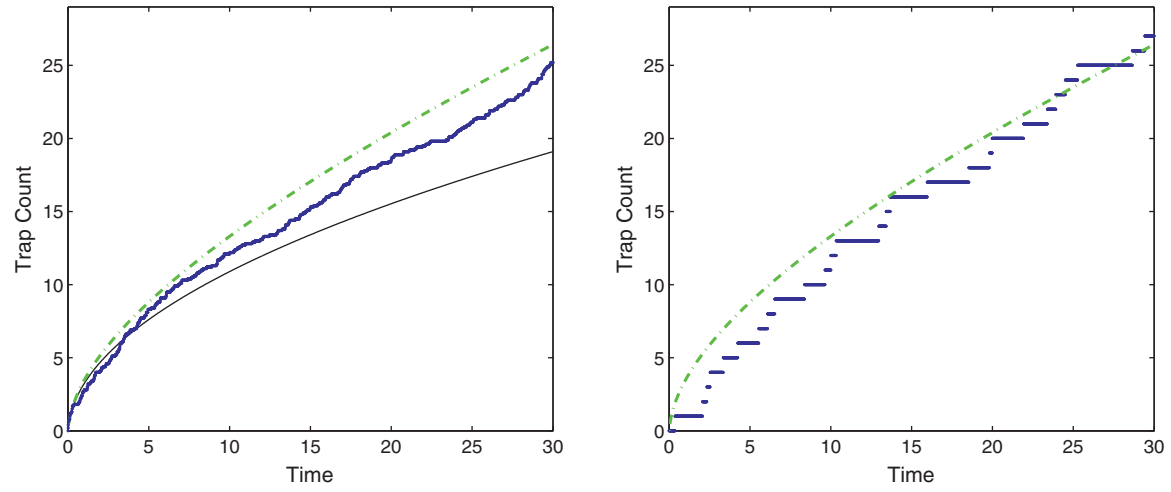

Fig. 13. Trap counts calculated using the individual-based approach (thick blue solid curve) and the scaled mean-field approach (green dashed-and-dotted curve), see Eq. (19): (left) averaged over 10 stochastic realizations, (right) for a typical stochastic realization. Parameters are $D = 1$, $n = 0.1$, $L = 50$ and $\kappa = 0.7$. The black solid curve shows the unscaled mean-field result given by (17). (For interpretation of the references to color in this figure legend, the reader is referred to the web version of the article.)

linear size of the region affected by diffusion as $r(t)$, then $A_{cr}(t) \sim pr(t)$ while $A_{tot}(t) \sim \pi r^2(t)$.

Taking into account that $r(t) \sim \sqrt{Dt}$ (see Appendix A), from (18) the following estimate is obtained:

$$(\Delta N)_t^* \approx p(\Delta N)_t \left(1 + \frac{\kappa\pi}{p}\sqrt{Dt}\right). \tag{19}$$

The contribution of the second term in the parentheses is therefore negligible at small t but becomes important at large t.

Note that, since it has been shown above that the shape of the trap is not important, Eq. (19) is expected to be applicable to describe trap counts by a circular-shaped trap as well. Figs. 12 and 13 show the comparison between the trap counts obtained in individual-based simulations (blue curve) with a circular trap and the trap counts calculated using (19) (green curve) with $(\Delta N)_t$ given by the exact solution (27). It is readily seen that the heuristic estimate (19) is in an excellent agreement with the simulation data when the population density is not too small (see Fig. 12). The agreement becomes somewhat worse for a smaller population density (Fig. 13) because of the increased magnitude of stochastic fluctuations. Even in the latter case, however, Eq. (19) correctly reproduces the tendency in the trap counts' growth over time.

5. Conclusions and discussion

Traps are commonly used in ecology, especially in insect studies, whenever the question arises about the abundance of a given species. Surprisingly, the methods to interpret the trap counts in order to derive an estimate of the population density in the field remain dramatically under-developed. In this paper, we have addressed this problem theoretically using a first-principle approach which considers insect movement as a stochastic process known as Brownian motion. The methods that are developed here are general and can be applied to any insect species and/or to any trap design, although the current focus of the work was mainly on walking/crawling insects and on non-baited trapping (e.g. by pitfall traps).

We have used this theoretical approach in two different ways. Firstly, having defined the probability distribution for the step size along the track, it is possible to simulate both the movement of a specific individual and the distribution of the population in space. Correspondingly, it becomes possible to simulate the trap counts

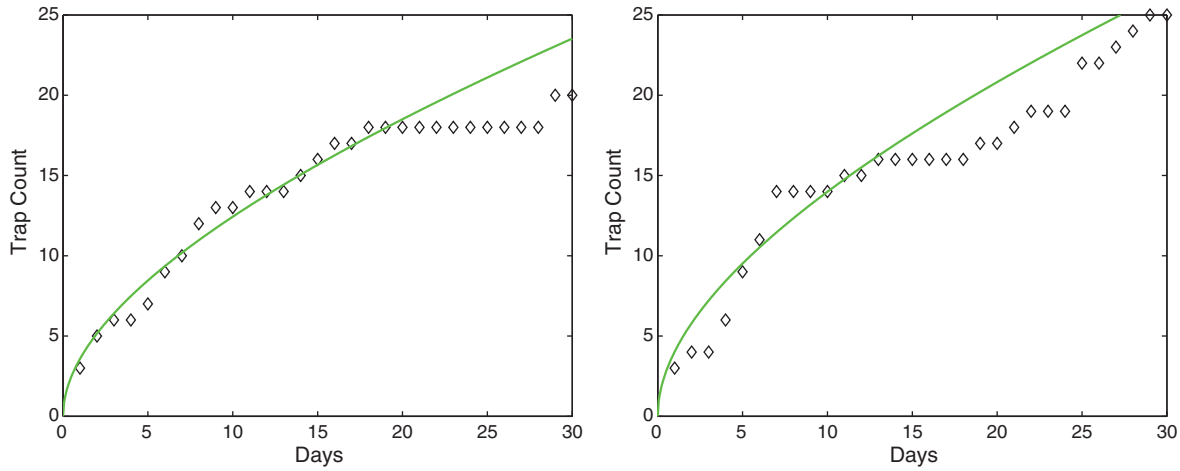

Fig. 14. Diamonds show two sample trap count sequences, Sample 1 (left) and Sample 2 (right), simulated by the individual-based approach for a circular trap of radius $R = 5$ installed in the center of a square-shaped field of size $L = 50$, other parameters are $D = 1$, $n = 0.1$ and $\kappa = 0.7$. The solid green curves show the best-fit obtained by nonlinear regression using the first 10 points in the dataset; the corresponding estimates for the population density are shown in Table 1. (For interpretation of the references to color in this figure legend, the reader is referred to the web version of the article.)

and to reveal a typical pattern in the trap catches for different insect mobility and different values of the population density. In doing that, it is assumed that the domain is isolated so that the insects cannot leave it and, even more importantly, there is no immigration from outside. It is also assumed that the initial distribution of insects is spatially homogeneous. Secondly, the simulation-based approach is complemented by a mean-field approach when the population is described in terms of its density rather than considering each individual track. In the case when individual insects perform the Brownian movement, the population density appears to be a solution of the diffusion equation. We have studied the properties of the diffusion equation subject to relevant boundary and initial conditions and compared them with the simulation results.

We have used a combination of these two approaches in order to reveal the generic properties of trap counts and to develop a conceptual framework that can be used to analyze the trapping data collected in the field. The main results of our study are as follows:

- The trap introduce a perturbation into the otherwise uniform spatial distribution of insects, cf. Figs. 3 and 9, with the insect density being considerably smaller in the vicinity of the trap than in the far field. The radius of this perturbation grows in time.
- The diffusion equation is shown to predict the properties of the trap count sequences 'on average'. Thus, the diffusion equation can be used as a generic framework to describe the trap counts. Simple analytical formulae have been obtained to describe the trap counts with a very good accuracy, see Eqs. (10) and (19) and Appendix B, which gives the possibility of fast and effective trap count interpretation (see below).
- The magnitude of stochastic fluctuations in trap counts increase as the population density decreases. It may result in a persistent trap count growth over a relatively long time (e.g. see the middle part of Figs. 5b and 6d), which can be misinterpreted as evidence of population growth and hence may send a wrong message to pest control managers.
- The magnitude of stochastic fluctuations is shown to be decreased by averaging the trap counts over several traps installed in the same field, provided the insects spatial distribution can be regarded as homogeneous. The number of traps required to reduce the fluctuations depends on the population density and the spatial behaviour of the target insect.

Table 1
Estimates of the population density n by nonlinear regression applied to the sample data sets shown in Fig. 14 (left (Sample 1) and right (Sample 2)) using Eqs. (10) and (19) with parameters $D = 1, \kappa = 0.7, L = 50$ and $p = 2\pi R$ where $R = 5$.

	Sample 1				Sample 2			
Number of days	30	20	10	5	30	20	10	5
Population density	0.082	0.091	0.092	0.080	0.091	0.093	0.104	0.079

Apart from the above results, we also made an insight into the mobility-density issue. It is confirmed (see Fig. 7) that a change in the population density can be compensated by a change in the individual insect mobility. However, it is also shown that the mobility-density relation is not straightforward: an m-fold increase in the insect density will have an effect on the trap counts significantly different from the corresponding m-fold increase in the insect mobility. Indeed, our theory predicts that the trap counts depend differently on the population density and on the mobility (as quantified by the diffusion coefficient D); see Eqs. (10) and (19). That opens up a possibility to separate the corresponding effects, although further research is needed to work out specific algorithms.

Now we are going to discuss in some more detail how our approach can be applied in practice to obtain an estimate of population density. Assume that we have got a trap count sequence. Fig. 14 shows two samples simulated by the individual-based approach (with $n = 0.1$, other parameters are given in the figure caption). How can the value of n can be restored from the data? The idea is that an estimate of n is provided by the best-fit of the data by analytical prediction (19). Examples of the best-fit curves (obtained by using nonlinear regression and standard software[4]) are shown in Fig. 14 and the corresponding estimates of n are given in Table 1. Therefore, our approach is capable of restoring the value of population density with a reasonable accuracy within 20%. Note that, in order to obtain a reliable estimate, it is not necessary to use a long trap count sequence: reducing the dataset to just the first five 'days' in the series will not make the accuracy much worse (see Table 1).

[4] We have used computational package NLREG © Phillip H. Sherrod; a demonstration version is available from http://www.nlreg.com and the algorithm description can be found in Dennis et al. (1981).

Thus, in this paper we have made the first step towards a consistent and predictive theory of insect trapping that makes it possible to relate the trap counts to the insect density. There remains a number of open questions. On the theoretical side, probably the most important question is what happens if insect movement is not exactly Brownian but shows a more complicated pattern such as, for instance, a correlated random walk or Levy walk (cf. Kareiva and Shigesada, 1983; Turchin, 1998). On a more practical side, an important question is to what extent the trap counts can be affected by heterogeneity in the insects' spatial distribution (cf. Alexander et al., 2005) and by migrations through the field boundary. It is hardly possible to address this question in terms of the conceptual framework that we have developed here because the answer will likely depend on the landscape properties, on the type of the culture grown in the field and/or on the biological traits of the insects (Holland et al., 2005). Equally important can be the effect of weather conditions that is known to affect insect mobility (cf. Crozier, 2003). An impact of these factors should become a focus of a separate study.

Acknowledgement

This work was supported by the Leverhulme Trust through grant F/00-568/X.

Appendix A. Diffusion equation in 1D case

We first notice that the problem ((5)–(8)) is symmetric with respect to the origin. Therefore, it is sufficient to consider it for $x > 0$.

For convenience, we introduce a new coordinate:

$$\xi = x - l \quad \text{so that} \quad x = \xi + l. \tag{20}$$

It is readily seen that, in the new variables (ξ, t) where $0 < \xi < \tilde{\mathcal{L}} = L - l$, the diffusion equation has the same form:

$$\frac{\partial u(\xi,t)}{\partial t} = D\frac{\partial^2 u(\xi,t)}{\partial \xi^2}. \tag{21}$$

For notations simplicity, in the below the tilde is omitted.

Correspondingly, the boundary conditions are

$$\frac{\partial u(\mathcal{L},t)}{\partial \xi} = 0 \quad \text{and} \quad u(0,t) = 0, \tag{22}$$

and the initial condition is

$$u(\xi,0) = n \quad \text{for} \quad 0 < \xi < \mathcal{L}. \tag{23}$$

The solution to the problem ((21)–(23)) describes the dynamics of the population density on the right of the trap; the solution on the left of the trap is obtained by changing ξ to $-\xi$.

Applying the method of variables separation (e.g. Crank, 1975), we arrive at the solution in the following form:

$$u(\xi,t) = \frac{4n}{\pi}\sum_{k=0}^{\infty}\frac{1}{(2k+1)}\sin\left(\frac{(2k+1)\pi\xi}{2\mathcal{L}}\right)\exp\left(-\frac{(2k+1)^2\pi^2 Dt}{4\mathcal{L}^2}\right). \tag{24}$$

From (24), the diffusion flux at the trap boundary is obtained as

$$j(t) = D\left|\frac{\partial u(\xi,t)}{\partial \xi}\right|_{\xi=0} = \frac{2Dn}{\mathcal{L}}\sum_{k=0}^{\infty}\exp\left(-\frac{(2k+1)^2\pi^2 Dt}{4\mathcal{L}^2}\right). \tag{25}$$

The number of insects caught over time t of the trap exposure is then obtained as

$$(\Delta N)_t = \int_0^t j(\tau)d\tau, \tag{26}$$

which results in

$$(\Delta N)_t = \frac{8\mathcal{L}n}{\pi^2}\sum_{k=0}^{\infty}\frac{1}{(2k+1)^2}\left[1 - \exp\left(-\frac{(2k+1)^2\pi^2 Dt}{4\mathcal{L}^2}\right)\right], \tag{27}$$

where Ln is the total number of insects for $x > 0$ at $t = 0$.

The number of trapped insects $(\Delta N)_t$ as given by (27) is shown in Fig. 15 by the solid curve. Note that, since

$$\sum_{k=0}^{\infty}\frac{1}{(2k+1)^2} = \frac{\pi^2}{8}, \tag{28}$$

in the large-time limit $(\Delta N)_t \to Ln$, i.e. all insects are trapped.

Appendix B. Approximation for the diffusive flux

Eq. (27) is not very convenient for practical purposes because working with infinite sums is not easy. However, we can try to find a reasonable approximation of (27) by a simpler formula. In order to do this, we change summation to integration in the right-hand side of (27):

$$(\Delta N)_t \approx \frac{8\mathcal{L}n}{\pi^2}\cdot\frac{\sqrt{\alpha}}{2}\int_{\sqrt{\alpha}}^{\infty}\left(1 - e^{-z^2}\right)\frac{dz}{z^2}, \tag{29}$$

where $\alpha = \pi^2 Dt/(4\mathcal{L}^2)$ and the integral can be calculated by parts resulting in

$$\int_{\sqrt{\alpha}}^{\infty}\left(1 - e^{-z^2}\right)\frac{dz}{z^2} = \frac{1 - e^{-\alpha}}{\sqrt{\alpha}} + \sqrt{\pi}\left[1 - \Phi(\sqrt{\alpha})\right], \tag{30}$$

where Φ is the error function. From ((29) and (30)), we obtain:

$$(\Delta N)_t \approx \frac{4\mathcal{L}n}{\pi^2}\left[(1 - e^{-\alpha}) + \sqrt{\pi\alpha}(1 - \Phi(\sqrt{\alpha}))\right]. \tag{31}$$

The number of trapped insects as given by (31) is shown in Fig. 15 by the magenta dotted curve. Therefore, Eq. (31) provides a good approximation to the exact solution (27) at a sufficiently small time (for up to $t \sim 5$ for parameters of Fig. 15); however, it significantly underestimates $(\Delta N)_t$ for larger t. Note that the larger the domain size L is the better approximation (31) works.

A closer look at the integral approximation reveals that most of the approximation error results from the first few terms in the series (27). Correspondingly, a much better result can be achieved if we keep the first term explicitly and change summation to integration in the remaining series:

$$\begin{aligned}(\Delta N)_t &\approx \frac{8\mathcal{L}n}{\pi^2}\left[(1 - e^{-\alpha}) + \frac{\sqrt{\alpha}}{2}\int_{3\sqrt{\alpha}}^{\infty}\left(1 - e^{-z^2}\right)\frac{dz}{z^2}\right] \\ &= \frac{8\mathcal{L}n}{\pi^2}\left((1 - e^{-\alpha}) + \frac{1}{6}(1 - e^{-9\alpha}) + \frac{\sqrt{\pi\alpha}}{2}\left[1 - \Phi(3\sqrt{\alpha})\right]\right).\end{aligned} \tag{32}$$

The trap count given by (32) is shown in Fig. 15 by the blue dashed-and-dotted curve.

A still better result is obtained if we keep the first and second term in the series (27) and change summation to integration in the remaining part:

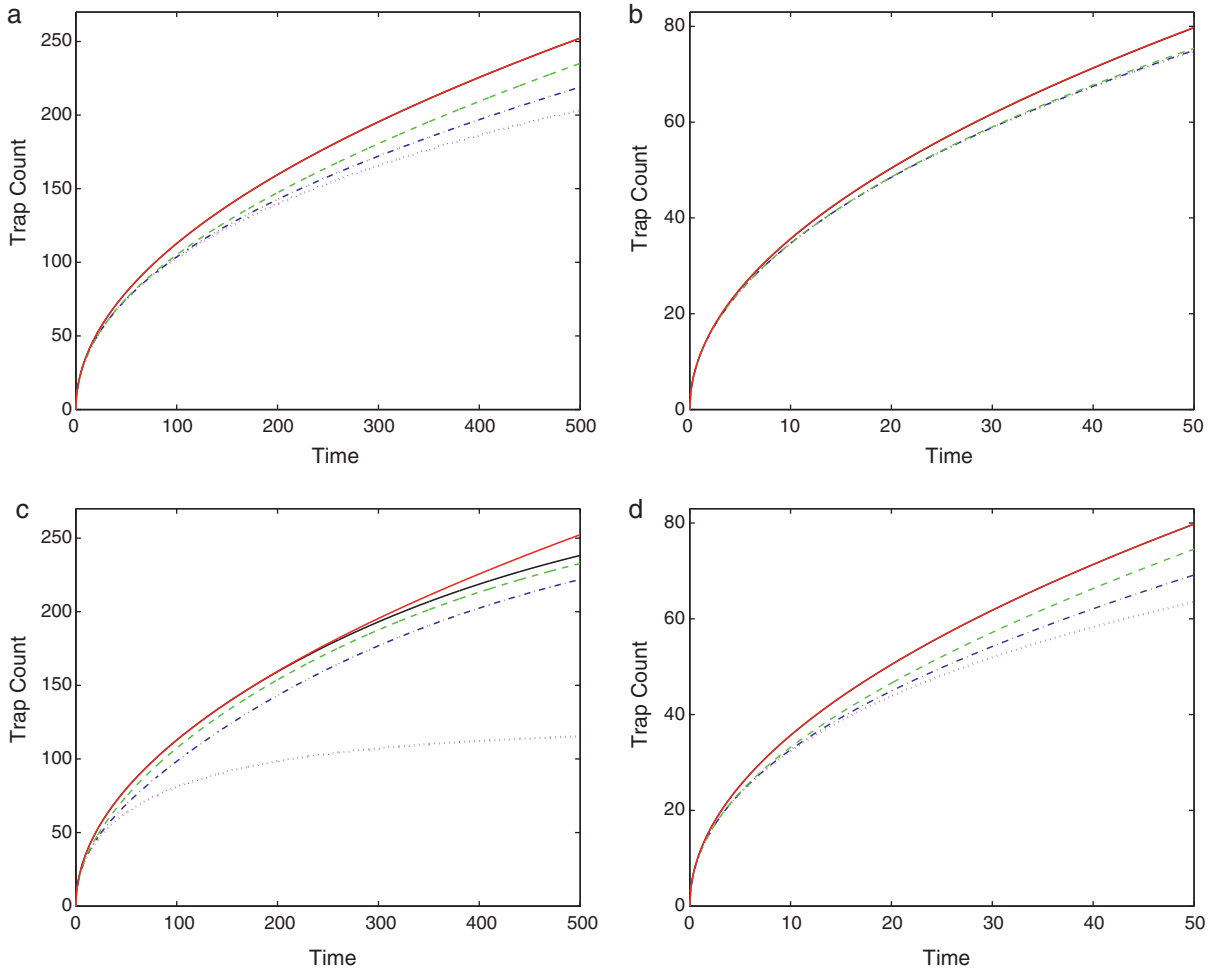

Fig. 15. Trap count vs. time shown over long (a and c) and short (b and d) time range as given by the exact solution (24) (black solid curve) and by its approximations (31) (magenta dotted curve), (32) (blue dashed-and-dotted curve), (33) (green dashed curve) and the square root approximation (34) (red solid curve). The domain size $\mathcal{L} = 100$ for (a and b) and $\mathcal{L} = 30$ for (c and d). Other parameters are $D = 1$ and $n = 10$. Note that red and black curves coincide everywhere except case (c). (For interpretation of the references to color in this figure legend, the reader is referred to the web version of the article.)

$$(\Delta N)_t \approx \frac{8\mathcal{L}n}{\pi^2}\left[(1-e^{-\alpha})+\frac{1}{9}(1-e^{-9\alpha})+\frac{\sqrt{\alpha}}{2}\int_{5\sqrt{\alpha}}^{\infty}\left(1-e^{-z^2}\right)\frac{dz}{z^2}\right]$$
$$=\frac{8\mathcal{L}n}{\pi^2}\left((1-e^{-\alpha})+\frac{1}{9}(1-e^{-9\alpha})+\frac{1}{10}(1-e^{-25\alpha})\right.$$
$$\left.+\frac{\sqrt{\pi\alpha}}{2}\left[1-\Phi(5\sqrt{\alpha})\right]\right). \qquad (33)$$

The trap count given by (33) is shown in Fig. 15 by the green dashed curve. Thus, although the last expression is rather bulky, it ensures that the approximation error remains within just a few percent over a very long time of the trap exposure.

Recall that we are mostly interested in the system's properties at small t. We therefore consider $\alpha \ll 1$. It is readily seen that, for small α, all three approximate expressions for the trap count obtained above are equivalent to

$$(\Delta N)_t = \frac{4\mathcal{L}n}{\pi^2}\sqrt{\pi\alpha}+O(\alpha) \approx \frac{4\mathcal{L}n}{\pi^2}\sqrt{\pi\alpha} = \frac{2n}{\sqrt{\pi}}\sqrt{Dt}, \qquad (34)$$

where $o(\alpha)$ stands for all higher order terms. Interestingly, although the approximate relation (34) is formally obtained under assumption $\alpha \ll 1$, it appears to be in an excellent agreement with the exact solution up to $\alpha \sim 1$. However, in case of slow moving insects (small D) in a large field (large $\mathcal{L}$), the square root approximation (34) can be valid over a very long time, as is indeed shown in Fig. 15.

It is readily seen that relation (34) becomes exact equality in case of a semi-infinite domain, i.e. when $\mathcal{L} \to \infty$. In that case, (34) is valid for any finite t.

References

Alexander, C.J., Holland, J.M., Winder, L., Wooley, C., Perry, J.N., 2005. Performance of sampling strategies in the presence of known spatial patterns. Ann. Appl. Biol. 146, 361–370.

Balescu, R., 1975. Equilibrium and Nonequilibrium Statistical Mechanics. John Wiley, New York.

Barenblatt, G.I., 1996. Scaling, Self-Similarity, and Intermediate Asymptotics. Cambridge University Press, Cambridge.

Begon, M., Townsend, C.R., Harper, J.L., 1986. Ecology: From Individuals to Ecosystems. Blackwell, Oxford.

Berg, H.C., 1983. Random Walks in Biology. Princeton University Press, Princeton.

Blackshaw, R.P., Vernon, R.S., 2008. Spatial relationships between two Agriotes click-beetle species and wireworms in agricultural fields. Agric. For. Ent. 10, 1–11.

Cain, M.L., Bowman, W.D., Hacker, S.D., 2011. Ecology, 2nd ed. Sinauer, Sunderland.

Chorin, A.J., Hald, O.H., 2006. Stochastic Tools in Mathematics and Science. Springer, New York.

Cochran, W.G., 1977. Sampling Techniques. John Wiley & Sons, New York.

Crank, J., 1975. The Mathematics of Diffusion, 2nd ed. Oxford University Press, Oxford.

Crozier, S., 2003. Flight activity of Agriotes lineatus L. and A. obscurus L. (Coleoptera: Elateridae) in the field. J. Ent. Soc. Br. Col. 100, 91–93.

Dennis, J.E., Gay, D.M., Welsch, R.E., 1981. An adaptive nonlinear least-squares algorithm. ACM Trans. Math. Softw. 7 (3).

Grimm, V., Railsback, S.F., 2005. Individual-based Modeling and Ecology. Princeton University Press, Princeton.

Hicks, H., Blackshaw, R.P., 2008. Differential responses of three Agriotes click beetle species to pheromone traps. Agric. For. Ent. 10, 443–448.
Holland, J.M., Thomas, C.F.G., Birkett, T., Southway, S., Oaten, H., 2005. Farm-scale spatiotemporal dynamics of predatory beetles in arable crops. J. Appl. Ecol. 42, 1140–1152.
Kareiva, P.M., Shigesada, N., 1983. Analyzing insect movement as a correlated random walk. Oecologia 56, 234–238.
Kot, M., 2001. Elements of Mathematical Ecology. Cambridge University Press, Cambridge.
Okubo, A., 1980. Diffusion and Ecological Problems: Mathematical Models. Springer, Berlin.
Perner, J., Schüler, S., 2004. Estimating the density of ground-dwelling arthropods with pitfall traps using a Nested-Cross array. J. Anim. Ecol. 73, 469–477.
Petrovskii, S.V., Morozov, A.Y., 2009. Dispersal in a statistically structured population: fat tails revisited. Am. Nat. 173, 278–289.
Petrovskii, S.V., Mashanova, A., Jansen, V.A.A., 2011. Variation in individual walking behavior creates the impression of a Lévy flight. PNAS 108, 8704–8707.
Raworth, D.A., Choi, W.-J., 2001. Determining numbers of active carabid beetles per unit area from pitfall-trap data. Ent. Exp. Appl. 98, 95–108.
Royama, T., 1982. Analytical Population Dynamics. Chapman & Hall, London.
Seber, G.A., 1982. The Estimation of Animal Abundance and Related Parameters. Charles Griffin, London.
Sornette, D., 2004. Critical Phenomena in Natural Sciences, 2nd ed. Springer, Berlin.
Stern, V.M., 1973. Economic thresholds. Annu. Rev. Entomol. 18, 259–280.
Sutherland, W.J. (Ed.), 1996. Ecological Census Techniques: A Handbook. Cambridge University Press, Cambridge.
Thomas, C.F.G., Parkinson, L., Marshall, E.J.P., 1998. Isolating the components of activity-density for the carabid beetle Pterostichus melanarius in farmland. Oecologia 116, 103–112.
Turchin, P., 1998. Quantitative Analysis of Movement. Sinauer, Sunderland.
Yamanaka, T., Tatsuki, S., Shimada, M., 2003. An individual-based model for sex-pheromone-oriented flight patterns of male moths in a local area. Ecol. Model. 161, 35–51.